

# Spectroscopic Investigation of *cis*-2,4-Difluorophenol Cation by Mass-analyzed Threshold Ionization Spectroscopy<sup>†</sup>

Vidya Shivatare<sup>‡,§</sup> and Wen Bih Tzeng<sup>§,\*</sup>

<sup>‡</sup>Molecular Science and Technology, Taiwan International Graduate Program Academia Sinica, 128 Academia Road, Nankang, Taipei 115, Taiwan

<sup>§</sup>Institute of Atomic and Molecular Sciences, Academia Sinica, P.O. Box 23-166, 1, Section 4, Roosevelt Road, Taipei 10617, Taiwan. \*E-mail: [wbt@sinica.edu.tw](mailto:wbt@sinica.edu.tw)

Received September 17, 2013, Accepted September 27, 2013

We applied the two-color resonant two-photon ionization and mass-analyzed threshold ionization techniques to record the vibronic and cation spectra of 2,4-difluorophenol. As supported by our theoretical calculations, only the *cis* form of 2,4-difluorophenol involves in the two-photon photoexcitation and pulsed field ionization processes. The band origin of the  $S_1 \leftarrow S_0$  electronic transition of *cis*-2,4-difluorophenol appears at  $35\,647 \pm 2\text{ cm}^{-1}$  and the adiabatic ionization energy is determined to be  $70\,030 \pm 5\text{ cm}^{-1}$ , respectively. Most of the observed active vibrations in the electronically excited  $S_1$  and cationic ground  $D_0$  states mainly involve in-plane ring deformation vibrations. Comparing these data of *cis*-2,4-difluorophenol with those of phenol, *cis*-2-fluorophenol, and 4-fluorophenol, we found that there is an additivity rule associated with the energy shift resulting from the additional fluorine substitution.

**Key Words :** Cation spectroscopy, Threshold ionization, Resonant ionization, *cis*-2,4-Difluorophenol

## Introduction

Fluorine substitution is a widely used strategy in the drug development because it alters the chemical properties, disposition, and biological activity of drugs.<sup>1-3</sup> Many fluorinated benzene derivatives,<sup>4-16</sup> are extensively studied by various spectroscopic methods. 2-Fluorophenol is regarded as one of the classic example of intramolecular hydrogen-bonding systems which have been the subject of various studies.<sup>6-12</sup> Chakrabarti *et al.* applied radiofrequency-microwave double resonance (RFMWDR) and conventional microwave spectroscopic techniques to record the microwave rotational spectra of gas-phase 2,4-difluorophenol (24DFP) in the ground  $S_0$  state.<sup>13</sup> They proposed that the *cis* and *trans* rotamers of 24DFP coexist and possess the intramolecular OH...F bonding, as that observed in 2-fluorophenol.<sup>8,12,14</sup> In addition, the *cis* form is more abundant than the *trans* form. Anbarasan and coworkers recorded the infrared and Raman spectra of 24DFP in the condensed phase and reported the active vibrations of this molecule in the  $S_0$  state.<sup>15</sup> They also performed the quantum chemical calculations to support their experimental results.<sup>15</sup> The ionization energy (IE) of this molecule has been reported on the basis of the conventional photoelectron spectroscopic experiments.<sup>16</sup> To the best of our knowledge, detailed spectroscopic data about the 24DFP in electronically excited  $S_1$  and cationic ground  $D_0$  state are not yet available in the literature. Both zero-kinetic energy (ZEKE) photoelectron and mass-analyzed threshold ionization (MATI) spectroscopic<sup>17-23</sup> techniques can provide in-

formation about the precise IE and active cation vibrations in the  $D_0$  state. The latter method provide mass information and is suitable for studies of radicals, complexes, clusters, or molecular systems in which impurities may be present. The one photon vacuum ultraviolet (VUV) MATI method is very useful to probing ionic properties of molecular systems whose electronic states cannot be reached by typical UV lasers or have short lifetime.<sup>24-26</sup> For many benzene derivatives whose first electronic transition can be reached by typical UV lasers, one can couple the resonant two-photon excitation scheme with the MATI technique. This approach has an advantage of species selection and is useful for studying cations of molecular conformers.<sup>24,25</sup>

In this paper, we report the vibronic and cation spectra of *cis*-24DFP, which were recorded by using the resonant two-photon ionization (R2PI) and MATI techniques. These new data provide information about the precise excitation energy of the  $S_1 \leftarrow S_0$  transition ( $E_1$ ) and adiabatic IE as well as the active vibrations in the  $S_1$  and cationic ground  $D_0$  state. By comparing the experimental data of *cis*-24DFP with those of some fluorine substituted phenol<sup>14,16,27,28</sup> and aniline derivatives,<sup>29-33</sup> we can learn about the substitution effects of the two F atoms on the transition energy and molecular vibration.

## Experimental and Computational

The present experiments were performed by using a coaxial laser based time-of-flight mass spectrometer equipped with two tunable UV lasers, as described in our previous publication.<sup>32</sup> 24DFP (99% purity) was purchased from Aldrich Corporation and used without further purification. The vapors of the sample were seeded into 2-3 bar of helium

<sup>†</sup>This paper is to commemorate Professor Myung Soo Kim's honourable retirement.

and expanded into the vacuum through a pulsed valve with a 0.15 mm diameter orifice. The molecular beam was collimated by a skimmer located 15 mm downstream from the nozzle orifice. A delay/pulse generator (Stanford Research Systems DG535) was used to control the two independent tunable UV laser to initiate the two-color resonant two-photon excitation process. A laser wavelength meter (Coherent, WaveMaster) was used to calibrate the wavelengths of both lasers. These two counter-propagating laser beams were focused and intersected perpendicularly with the molecular beam at 50 mm downstream from the nozzle orifice. During the experiments, the gas expansion, laser-molecular beam interaction, and ion detection regions are maintained at a pressure of about  $1 \times 10^{-3}$ ,  $1 \times 10^{-5}$ , and  $1 \times 10^{-6}$  Pa (*i.e.*  $1 \times 10^{-5}$ ,  $1 \times 10^{-7}$ , and  $1 \times 10^{-8}$  mbar), respectively.

In the MATI experiments, both prompt ions and Rydberg neutrals were formed simultaneously in the laser-molecular beam interaction zone. A pulsed electric field of  $-1$  V/cm (duration = 10  $\mu$ s) in this region (Region I) was applied about 135 ns after the occurrence of the laser pulses to guide the prompt ions towards the opposite direction of the flight tube.<sup>32</sup> In this way, the prompt ions were not detected by the particle detector. Because the Rydberg neutrals were not affected by the electric field, they kept moving with molecular beam velocity of about 1500 m/s to enter the field-ionization region (Region II).<sup>32</sup> After a time delay of about 11.8  $\mu$ s, a second pulsed electric field of +200 V/cm was turned to field-ionize the Rydberg neutrals. The threshold ions were then accelerated and passed a 1.0 m field-free region before being detected by a dual-stack microchannel plate particle detector. The ion signal from the detector was collected and analyzed by a multichannel scaler (MCS, Stanford Research System, SR430) which was interfaced to a personal computer. Mass spectra were accumulated at 1.2  $\text{cm}^{-1}$  spacing for 300 laser shots. Composite optical spectra of intensity *versus* wavelength were then constructed from the individual mass spectra. As the detected signal is proportional to the photon intensities of the excitation and ionization lasers for a two-color two-photon process, the obtained optical spectra were normalized to the laser power in order to avoid spurious signals due to shot-to-shot laser fluctuation.

We have performed *ab initio* and density functional theory (DFT) calculations by using the GAUSSIAN 09 program package.<sup>34</sup> The calculated results can provide information about the total energies, structures, vibrational frequencies, and many other molecular properties of 24DFP in the  $S_0$ ,  $S_1$ , and  $D_0$  states. The spin multiplicity  $\langle S^2 \rangle$  has been checked to be 0.75 for the cation. The computed vibrational frequencies are multiplied by a suitable factor and used to assign the vibronic and MATI spectra. The IE was deduced from the difference of the zero-point energies (ZPEs) of the cation in the  $D_0$  state and the corresponding neutral species in the  $S_0$  state.

## Results

### Vibronic Spectra.

We have applied both one-color (1C)

and two-color (2C) resonant two photon ionization (R2PI) techniques to record the vibronic spectra of 24DFP, as shown in Figure 1. Under the experimental conditions of the 1C-R2PI process, the excess energy is estimated to be about 1260–3160  $\text{cm}^{-1}$  for the spectral range shown in Figure 1(a). The 2C-R2PI experiments were performed by scanning the excitation laser while fixing the ionization laser at 290 nm. For the entire spectral range, the largest excess energy is no more than 1100  $\text{cm}^{-1}$ . Under this experimental condition, no fragment ion signal appears in the TOF mass spectrum. This allows us to record the vibronic spectrum of 24DFP with good quality. Although the 2C-R2PI spectrum has a slightly better signal-to-noise ratio, the general vibronic features of both spectra are nearly identical. It is noted that a few vibronic bands (*e.g.*  $10b^2_0$ ,  $9a^1_0$ , and  $1^1_0$ ) in the 2C-R2PI spectrum have slightly lower intensity than the corresponding ones in the 1C-R2PI spectrum. A possible reason is that the lifetimes of these vibronic states are comparable to or slightly shorter than the pulse duration (4–6 ns) of our pump and probe lasers. Detailed investigation may be conducted in the future. The band origin of the  $S_1 \leftarrow S_0$  electronic excitation ( $E_1$ ) of 24DFP appears at  $35\,647 \pm 2$   $\text{cm}^{-1}$ . Similar to the case of 2-fluorophenol,<sup>8,9,14</sup> only one stable *cis* conformation of 24DFP is found to be involved in the present R2PI and MATI experiments, as predicted by the theoretical calculations. In addition to the optimized structure, the

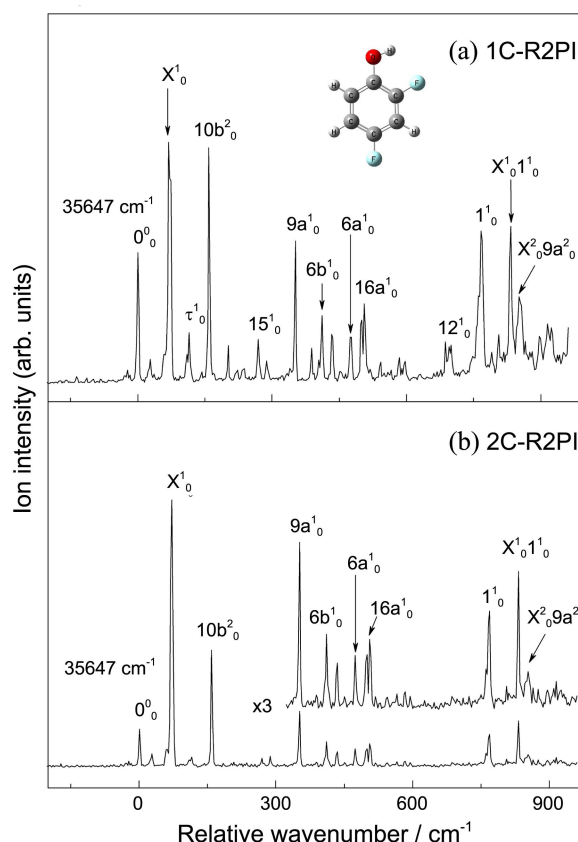


**Figure 1.** Vibronic spectra of *cis*-24DFP recorded by the (a) 1C-R2PI and (b) 2C-R2PI methods. The 2C-R2PI spectrum was obtained by scanning the pump laser while fixing the probe laser at 290 nm.

**Table 1.** Observed bands in the vibronic spectrum of *cis*-24DFP<sup>a</sup>

Energy (cm <sup>-1</sup> )	Shift (cm <sup>-1</sup> )	Cal. (cm <sup>-1</sup> )		Assignment <sup>b</sup>
		CIS	B3PW91	
35 647	0			origin
35 719	72			X <sub>1</sub> <sup>0</sup>
35 806	159	176	150	10b <sup>2</sup> <sub>0</sub> , γ(C–OH), γ(CF)
35 849	202	186		10a <sup>1</sup> <sub>0</sub> , γ(CH)
35 916	269	286	246	15 <sup>1</sup> <sub>0</sub> , β(CF), β(CO)
35 999	352	347	354	9a <sup>1</sup> <sub>0</sub> , β(CF), β(CO)
36 059	412	414	381	6b <sup>1</sup> <sub>0</sub> , β(CCC)
36 647	433			X <sub>1</sub> <sup>0</sup> 9a <sup>1</sup> <sub>0</sub>
36 121	474	447	451	6a <sup>1</sup> <sub>0</sub> , β(CCC)
36 147	500			X <sub>2</sub> <sup>0</sup> 9a <sup>1</sup> <sub>0</sub>
36 153	506	512	517	16b <sup>1</sup> <sub>0</sub> , γ(CCC)
36 341	694	690	677	12 <sup>1</sup> <sub>0</sub> , β(CCC)
36 416	766		768	1 <sup>1</sup> <sub>0</sub> , breathing
36 480	832			X <sub>1</sub> <sup>0</sup> 1 <sup>1</sup> <sub>0</sub>
36 498	851			X <sub>2</sub> <sup>0</sup> 9a <sup>2</sup> <sub>0</sub>

<sup>a</sup>The experimental values are shifts from 35 647 cm<sup>-1</sup>, whereas the calculated ones are obtained from the CIS (scaled by 0.92) and B3PW91 calculations using the 6-311++G(d,p) basis set. <sup>b</sup>β, in-plane bending; γ, out-of-plane bending.

electronic excitation energy can be estimated by various theoretical calculations. The configuration interaction singles (CIS), and time-dependent Becke three-parameter with the PW91 correlation functional (TD-B3PW91) with the 6-

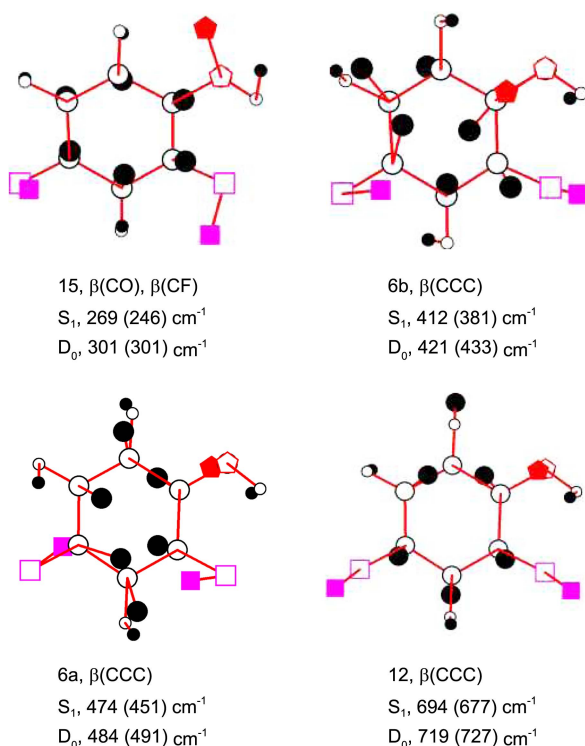


**Figure 2.** Some observed active vibrations of *cis*-24DFP in S<sub>1</sub> and D<sub>0</sub> states. The open circles designate the original locations of the atoms, whereas the solid dots mark the displacements. The measured and calculated (in the parentheses) frequencies are included for each mode.

311++G(d,p) basis set predict the E<sub>1</sub>'s to be 45 705 and 36 594 cm<sup>-1</sup>, corresponding to overestimations of 28 and 2.7%, respectively.

The observed vibronic bands of *cis*-24DFP are listed in Table 1. The spectral assignment was done by comparing the present data with the experimental values of phenol,<sup>27</sup> *cis*-2-fluorophenol,<sup>14</sup> 4-fluorophenol,<sup>28</sup> and 2,4-difluoroaniline,<sup>33</sup> as well as the predicted vibrational frequencies from the CIS and TD-B3PW91/6-311++G(d,p) calculations. The intense low-frequency bands at 72 and 159 cm<sup>-1</sup> result from vibronic transitions related to out-of-plane bending vibrations X<sub>1</sub><sup>0</sup> and 10b<sup>2</sup><sub>0</sub>, respectively. A similar X<sub>1</sub><sup>0</sup> band at 87 cm<sup>-1</sup> has been reported for, 2,4-difluoroaniline.<sup>33</sup> In previous studies of *cis*-2-fluorophenol,<sup>12,14</sup> the strong vibronic band at 109 cm<sup>-1</sup> was assigned to the overtone transition related to an out-of-plane “butterfly” vibration. The distinct bands at 269 and 352 cm<sup>-1</sup> correspond to transitions related to the substituent-sensitive in-plane CF and CO bending vibrations 15 and 9a, whereas those at 766, 412, 474, and 694 cm<sup>-1</sup> result from the in-plane deformation modes 1, 6b, 6a, and 12, respectively. The weak band at 506 cm<sup>-1</sup> is tentatively assigned to transition related to out-of-plane ring deformation vibration 16b. Some of the active vibration modes are shown in Figure 2.

**Cation Spectra.** We performed both the photoionization

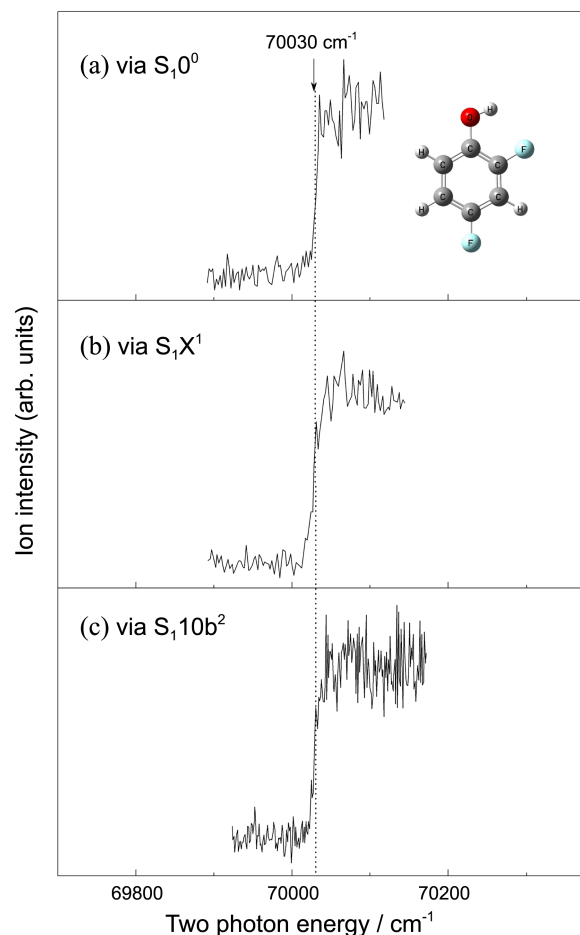


**Figure 3.** PIE curves of *cis*-24DFP recorded by ionizing via the (a) S<sub>1</sub>0<sup>0</sup>, (b) S<sub>1</sub>X<sup>1</sup>, (c) S<sub>1</sub>10b<sup>2</sup> states, respectively.

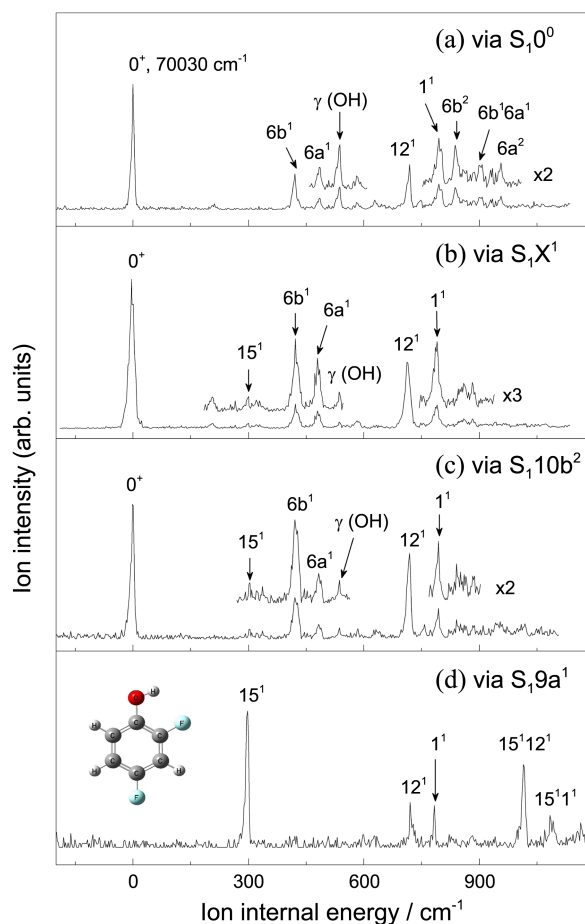


**Figure 4.** MATI spectra of *cis*-24DFP recorded by ionizing *via* the (a)  $S_1 0^0$ , (b)  $S_1 X^1$ , (c)  $S_1 10b^2$ , and (d)  $S_1 9a^1$  states, respectively.

efficiency (PIE) and MATI experiments to investigate the ionic properties of *cis*-24DFP. The PIE experiment involves detection of total ion currents and leads to an abruptly rising step near the ionization limit. It is noted that the present 2C-R2PI procedure for recording the PIE curve is different from that for recording the vibronic spectrum stated previously. This 2C-R2PI procedure is accomplished by scanning the ionization laser while fixing the frequency of the excitation laser at specific vibronic levels of the molecular species. Figure 3 shows the PIE curves obtained by ionizing *via* the  $S_1 0^0$  ( $35\,647\text{ cm}^{-1}$ ),  $S_1 X^1$  ( $35\,719\text{ cm}^{-1}$ ), and  $S_1 10b^2$  ( $35\,806\text{ cm}^{-1}$ ) levels of *cis*-24DFP. In all these three PIE curves, the abruptly rising step at  $70\,030 \pm 10\text{ cm}^{-1}$  indicates the IE of this molecule. The MATI experiment involves detection of the threshold ions formed by pulsed field ionization and gives a sharp peak at the ionization limit. The major advantage of this method is that it provides information about the ion internal energy. Figure 4 displays the MATI spectra of *cis*-24DFP recorded by ionizing *via* the  $S_1 0^0$  ( $35\,647\text{ cm}^{-1}$ ),  $S_1 X^1$  ( $0^0+72\text{ cm}^{-1}$ ),  $S_1 10b^2$  ( $0^0+159\text{ cm}^{-1}$ ), and  $S_1 9a^1$  ( $0^0+352\text{ cm}^{-1}$ ) levels in the  $S_1$  state. Analysis of the sharp  $0^+$  bands gives the field-corrected adiabatic IE to be  $70\,030 \pm 5\text{ cm}^{-1}$  ( $8.6826 \pm 0.0006\text{ eV}$ ), which is in excellent agreement with that measured from our PIE experiments. Maier *et al.* report-

**Table 2.** Observed bands (in  $\text{cm}^{-1}$ ) in the MATI spectra of *cis*-24DFP<sup>a</sup>

$0^0$	Intermediate level in the $S_1$ state				Assignments <sup>b</sup>
	$X^1$	$10b^2$	$9a^1$	Cal.	
	301	301	299	301	$15^1$ , $\beta(\text{CO})$ , $\beta(\text{CF})$
421	421	421		433	$6b^1$ , $\beta(\text{CCC})$
484	484	484		491	$6a^1$ , $\beta(\text{CCC})$
538	537	537		592	$\gamma(\text{OH})$
719	719	719	720	727	$12^1$ , $\beta(\text{CCC})$
796	795	795	789	803	$1^1$ , breathing
838	840	840			$6b^2$
905					$6b^1 6a^1$
960					$6a^2$
			1019		$15^1 12^1$
			1084		$15^1 1^1$

<sup>a</sup>The experimental values are shifts from  $70\,030\text{ cm}^{-1}$ , whereas the calculated ones are obtained from the B3PW91/6-311++G(d,p) calculations. <sup>b</sup> $\beta$ , in-plane bending;  $\gamma$ , out-of-plane bending.

ed the IE of this molecule to be 8.98 eV by performing the conventional photoelectron spectroscopic experiments.<sup>16</sup> In addition to the precise IE value, the MATI spectra can provide information about the active vibrations of the cation. The observed MATI bands and their possible assignments are listed in Table 2. When the  $S_1 0^0$  is used as the intermediate state, the distinct bands at 421, 484, 719, and 796  $\text{cm}^{-1}$  in the MATI spectrum correspond to the in-plane ring deformation vibrations  $6b^1$ ,  $6a^1$ ,  $12^1$ , and  $1^1$  of the *cis*-24DFP cation, respectively. These  $6b^1$ ,  $6a^1$ , and breathing  $1^1$  vibrations were also found to be active with respective frequencies of 429, 539 and 715  $\text{cm}^{-1}$  for the 2,4-difluoroaniline cation.<sup>33</sup> Figure 4(b) and (c) depicts the MATI spectra recorded by ionizing *via* the  $S_1 X^1$  and  $S_1 10b^2$  intermediate levels, respectively. The strongest band appears at the ionization threshold. The distinct bands at 421, 719 and 796  $\text{cm}^{-1}$  result from vibrations  $6b^1$ ,  $12^1$ , and  $1^1$  respectively. Figure 4(d) shows the MATI spectrum recorded *via* the  $S_1 9a^1$  level. The in-plane ring deformation vibrations 15, 12, and 1 are found to have frequencies of 299, 720, and 789  $\text{cm}^{-1}$ , respectively.

## Discussion

Due to the relative orientation of the OH group with respect to the F atom, different rotamers of 24DFP may coexist in the sample. Chakrabarti and Jaman applied the conventional microwave spectroscopic technique to investigate the stable structure of 24DFP in the  $S_0$  state.<sup>13</sup> With help from theoretical calculations, they proposed that that presence of an intramolecular  $\text{OH}\cdots\text{F}$  bonding preferentially stabilizes the *cis* conformer of 24DFP, as that observed in 2-fluorophenol.<sup>8,12,14</sup> A similar observation has been reported for 2-fluorophenol<sup>14</sup> and 2-chlorophenol.<sup>35</sup>

We have performed the Becke three-parameter with the PW91 correlation functional (B3PW91) calculations with the 6-311++G(d,p) basis set to investigate the stable rotamers

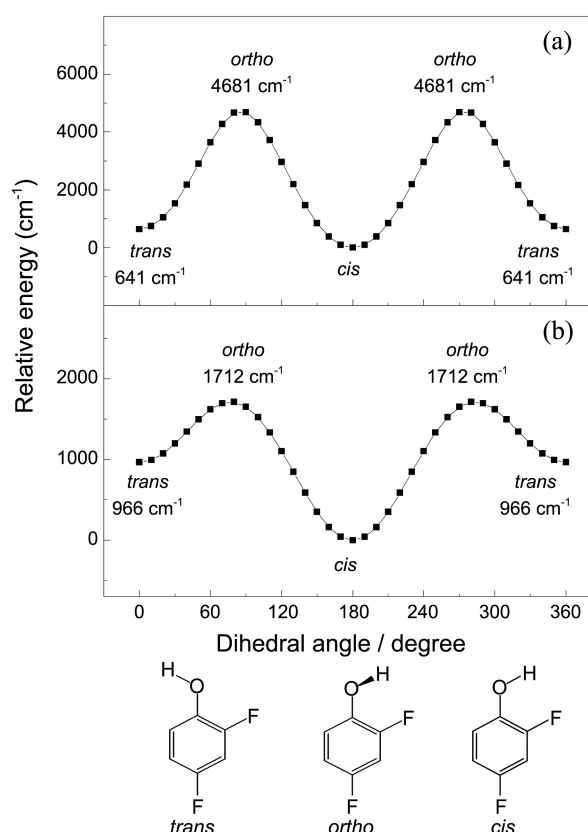


**Figure 5.** One-dimensional potential energy surfaces of 24DFP in the (a)  $D_0$  and (b)  $S_0$  states, obtained from the B3PW91 calculations with the 6-311++G(d,p) basis set.

of 24DFP in the  $S_0$ ,  $S_1$ , and  $D_0$  states respectively. These calculations were done by scanning the one-dimensional potential energy surface on the rotation of C–OH bond. The sum of electronic and zero-point energies of *cis*- and *trans*-24DFP in the  $S_0$  state are estimated to be  $-505.804917$  and  $-505.800808$  hartree, respectively. As seen in Figure 5(b), the *cis* conformer is the most stable species. In addition, the *trans* and *ortho* forms lie in higher energy levels by 966 and 1712  $\text{cm}^{-1}$  respectively. The same calculations for 2-fluorophenol<sup>14</sup> also predict the *cis* form is the most stable species and the *trans* form lies in a higher energy level by 917  $\text{cm}^{-1}$ . In the  $D_0$  state, the *cis* form of 24DFP is also the most stable species, whereas the *trans* form lies in a higher energy level by 641  $\text{cm}^{-1}$ , as seen in Figure 5(a). The energy barrier for isomerization between the *cis* and *trans* rotamers is predicted to be 746–1712  $\text{cm}^{-1}$  in the  $S_0$  state and 4040–4681  $\text{cm}^{-1}$  in the  $D_0$  state, respectively. The present calculated results suggest that only the *cis* form of 24DFP involves in the  $S_1 \leftarrow S_0$  electronic excitation and the  $D_0 \leftarrow S_1$  ionization processes.

Table 3 lists the measured  $E_1$ 's and IEs of phenol and its fluorine substituted derivatives on the basis of the REMPI and MATI experiments.<sup>14,27,28</sup> The  $E_1$  of *cis*-2-fluorophenol is greater than that of phenol by 455  $\text{cm}^{-1}$ , whereas those of 4-fluorophenol and *cis*-24DFP are less by 702  $\text{cm}^{-1}$  and 1232  $\text{cm}^{-1}$ , respectively. A substituent can interact with the aromatic ring by inductive effect through the  $\sigma$  bond or by

**Table 3.** Measured transition energies ( $\text{cm}^{-1}$ ) of phenol and its fluorine substituted derivatives<sup>a</sup>

Molecule	$S_1 \leftarrow S_0$	$\delta E_1$	$D_0 \leftarrow S_1$	$\delta E_2$	IE	$\delta \text{IE}$
Phenol <sup>b</sup>	36 349	0	32 276	0	68 625	0
2-Fluorophenol, <i>cis</i> <sup>c</sup>	36 804	455	33 202	926	70 006	1381
4-Fluorophenol <sup>d</sup>	35 117	-1232	33 460	1184	68 577	-48
2,4-Difluorophenol, <i>cis</i> <sup>e</sup>	35 647	-702	34383	2107	70 030	1405

<sup>a</sup> $\delta E_1$ ,  $\delta E_2$ , and  $\delta \text{IE}$  are shifts of the  $S_1 \leftarrow S_0$ ,  $D_0 \leftarrow S_1$ , and IE with respect to those of phenol. <sup>b</sup>Ref. 27. <sup>c</sup>Ref. 14. <sup>d</sup>Ref. 28. <sup>e</sup>This work.

resonance (or called mesomeric) effect through the overlap of  $\pi$  molecular orbitals. In addition, a substituent can interact with another substituent by through-space interaction. Because the substituent–ring and substituent–substituent interactions depend on the nature, location, and relative orientation of substituents, each factor can not be quantified. However, substitution of a functional group on the aromatic ring will lead to a lowering of the ZPE level of a molecule due to the collective result of these factors. The observed blue shift in the transition energy indicates that the degree of lowering of the ZPE level of the upper state is smaller than that of the lower state. Oppositely, a red shift in the transition energy implies that the magnitude of lowering of the ZPE level of the upper state is larger than that of the lower state. Huang and Lombardi<sup>36</sup> performed Stark effect experiments and found that the substituent–ring interactions of 4-fluorophenol in the  $S_1$  state is enhanced and has a quinoid-like resonance structure. It results in a red shift in the  $E_1$  of 4-fluorophenol with respect to phenol. When the fluorine atom locates at the *ortho* position, the collective inductive and resonance effects of the OH and F substituents lead to a blue shift in the  $E_1$ 's of *cis*-2-fluorophenol with respect to phenol, as seen in Table 3.

It is noted that the energy shift of 455  $\text{cm}^{-1}$  [for *cis*-2-fluorophenol] + (–1232  $\text{cm}^{-1}$ ) [for 4-fluorophenol] = –777  $\text{cm}^{-1}$  which deviates from the observed value of –702  $\text{cm}^{-1}$  for *cis*-24DFP by only 75  $\text{cm}^{-1}$ . Similar findings of an additivity propensity associated with the energy shift in the  $E_1$  has been reported for 2,4-difluoroaniline<sup>33</sup> and 3,4-difluoroanisole.<sup>37</sup>

We define  $E_2$  as the energy associated with the  $D_0 \leftarrow S_1$  transition process in a two-photon photoexcitation/ionization process. As seen in Table 3, the energy shift in the  $E_2$  of 926  $\text{cm}^{-1}$  [for *cis*-2-fluorophenol] + 1184  $\text{cm}^{-1}$  [for 4-fluorophenol] = 2110  $\text{cm}^{-1}$ , which deviates from the observed value of 2107  $\text{cm}^{-1}$  for *cis*-24DFP by 3  $\text{cm}^{-1}$ . The present two-color resonant two-photon MATI experiments involve both (1) the  $S_1 \leftarrow S_0$  electronic excitation and the (2) the  $D_0 \leftarrow S_1$  transition processes. The IE is the sum of  $E_1$  and  $E_2$ . One finds that the energy shift in the IE is as follows, 1381  $\text{cm}^{-1}$  [for *cis*-2-fluorophenol] + (–48)  $\text{cm}^{-1}$  [for 4-fluorophenol] = 1333  $\text{cm}^{-1}$ . This value only deviates from the observed value of 1405  $\text{cm}^{-1}$  for *cis*-24DFP by 72  $\text{cm}^{-1}$ . These data show that there is an additivity rule associated with the energy shift in the  $E_1$ ,  $E_2$ , and IE of *cis*-24DFP, as those reported for 2,4-difluoroaniline<sup>33</sup> and 3,4-difluoroanisole.<sup>37</sup>

Most of the active vibrations observed in R2PI and MATI spectra result from in-plane ring deformation and substituent-sensitive in-plane bending motions. The frequencies of in-plane ring deformation vibrations  $6b^1$ ,  $6a^1$ ,  $12^1$ , and  $1^1$  are found to be 412, 474, 694, and  $766\text{ cm}^{-1}$  in the  $S_1$  state and increase to be 421, 484, 719, and  $796\text{ cm}^{-1}$  for its cation in the  $D_0$  state respectively. The observation of the frequency difference in each mode of different states suggests that the geometry of *cis*-24DFP is slightly more rigid in the cationic  $D_0$  state than that in the neutral  $S_1$  state.

### Conclusion

We applied the R2PI and MATI techniques to record the vibrational spectra of *cis*-24DFP in the  $S_1$  and  $D_0$  states. The excitation energy of  $S_1 \leftarrow S_0$  excitation is found to be  $35\,647 \pm 2\text{ cm}^{-1}$ , whereas the IE is determined to be  $70\,030 \pm 5\text{ cm}^{-1}$ . Comparing these values with those of phenol, *cis*-2-fluorophenol, and 4-fluorophenol, we found that there is an additivity rule associated with the energy shifts in the  $E_1$ ,  $E_2$ , and IE of *cis*-24DFP. The present experimental results show that most of the observed active vibrations of *cis*-24DFP in the  $S_1$  and  $D_0$  states mainly involve in-plane ring deformation and substituent-sensitive in-plane bending motions, as those found in phenol, *cis*-2-fluorophenol, and 4-fluorophenol. In addition, investigations on the frequencies of the active vibrations suggest that the geometry of *cis*-24DFP is more rigid in the cationic  $D_0$  state than that in the neutral  $S_1$  state.

**Acknowledgments.** We gratefully acknowledge financial support from the National Science Council of the Republic of China under Grant NSC-102-2113-M-001-009. And the publication cost of this paper was supported by the Korean Chemical Society.

### References

1. Park, B. K.; Kitteringham, N. R.; O'Neill, P. M. *Annu. Rev. Pharmacol. Toxicol.* **2001**, 41, 443.
2. Strunecká, A.; Patočka, J.; Connett, P. J. *App. Biomedicine* **2004**, 2, 141.
3. Filler, R.; Saha, R. *Future Med. Chem.* **2009**, 1(5), 777.
4. Kwon, C. H.; Kim, H. L.; Kim, M. S. *J. Chem. Phys.* **2002**, 116, 10361.
5. Kwon, C. H.; Kim, H. L.; Kim, M. S. *J. Chem. Phys.* **2003**, 118, 6327.
6. Oikawa, A.; Abe, H.; Mikami, N.; Ito, M. *Chem. Phys. Lett.* **1985**, 116, 50.
7. Omi, T.; Shitomi, H.; Sekiya, M.; Takazawa, K.; Fujii, M. *Chem. Phys. Lett.* **1996**, 252, 287.
8. Fujimaki, E.; Fujii, A.; Ebata, T.; Mikami, N. *J. Chem. Phys.* **1999**, 110, 4238.
9. Fujii, A.; Iwasaki, A.; Mikami, N. *Chem. Lett.* **1997**, 11, 1099.
10. Baker, A. W.; Kaeding, W. W. *J. Am. Chem. Soc.* **1959**, 81, 5904.
11. Wu, R.; Brutschy, B. *Chem. Phys. Lett.* **2004**, 390, 272.
12. Remmers, K.; Meerts, W. L.; Zehnacker-Rentien, A.; Barbu, K. L.; Lahmani, F. *J. Chem. Phys.* **2000**, 112, 6237.
13. Chakrabarti, S.; Jaman, A. I. *J. Molec. Struct.* **2002**, 642, 93.
14. Yuan, L.; Li, C.; Lin, J. L.; Yang, S. C.; Tzeng, W. B. *Chem. Phys.* **2006**, 323, 429.
15. Subramanian, M. K.; Anbarasana, P. M.; Manimegalai, S. *J. Raman Spectrosc.* **2009**, 40, 1657.
16. Maier, J. P.; Marthaler, O.; Mohraz, M. *J. Electron Spectrosc. Related Phenomena* **1980**, 19, 11.
17. Park, S. T.; Kim, H. L.; Kim, M. S. *Bull. Korean Chem. Soc.* **2002**, 23, 1247.
18. Park, S. T.; Kim, S. K.; Kim, M. S. *Nature* **2002**, 415, 306.
19. Baek, S. J.; Choi, K. W.; Choi, Y. S.; Kim, S. K. *J. Chem. Phys.* **2002**, 117, 2131.
20. Zhu, L.; Johnson, P. J. *Chem. Phys.* **1991**, 94, 5769.
21. Müller-Dethlefs, K.; Sander, K. M.; Schlag, E. W. *Chem. Phys. Lett.* **1984**, 112, 291.
22. Cockett, M. C. R. *Chem. Soc. Rev.* **2005**, 34, 935.
23. Li, J.; Li, H.; Mo, Y. *J. Phys. Chem. A* **2010**, 114, 9973.
24. Park, S. T.; Kim, M. S. *J. Am. Chem. Soc.* **2002**, 124, 7614.
25. Dickinson, H.; Chelmick, T.; Softley, T. P. *Chem. Phys. Lett.* **2001**, 338, 37.
26. Kostko, O.; Kim, S. K.; Leone, S. R.; Ahmed, M. *J. Phys. Chem. A* **2009**, 113, 14206.
27. Dopfer, O.; Müller-Dethlefs, K. *J. Chem. Phys.* **1994**, 10, 8508.
28. Zhang, B.; Li, C.; Su, H.; Lin, J. L.; Tzeng, W. B. *Chem. Phys. Lett.* **2004**, 390, 65.
29. Lin, J. L.; Tzeng, W. B. *J. Chem. Phys.* **2001**, 115, 743.
30. Tzeng, W. B.; Narayanan, K.; Hsieh, C. Y.; Tung, C. C. *J. Chem. Soc. Faraday. Trans.* **1997**, 93, 2981.
31. Lin, J. L.; Tzeng, W. B. *Phys. Chem. Chem. Phys.* **2000**, 2, 3759.
32. Tzeng, W. B.; Lin, J. L. *J. Phys. Chem. A* **1999**, 103, 8612.
33. Huang, W. C.; Huang, P. S.; Hu, C. H.; Tzeng, W. B. *Spectrochim. Acta A* **2012**, 93, 176.
34. Frisch, M. J. *et al.* GAUSSIAN 09, Revision A.02, Gaussian, Inc., Pittsburgh, PA, 2009.
35. Onda, M.; Oshima, Y.; Yamaguchi, I. *Bull. Chem. Soc. Jpn.* **1978**, 51, 65.
36. Huang, K. T.; Lombardi, J. R. *J. Chem. Phys.* **1969**, 51, 1228.
37. Xu, Y.; Tzeng, S. Y.; Zhang, B.; Tzeng, W. B. *Spectrochim. Acta A* **2013**, 102, 365.